Int. J. Electrochem. Sci., 10 **(2015)** 1979 - 1991

International Journal of
ELECTROCHEMICAL
SCIENCE
www.electrochemsci.org

Electrochemical Behavior of Nickel in the EMIC Ionic Liquid with Glycol

Yingya Yang[1], *Cunying Xu*[1,2,*], *Yixin Hua*[1,2], *Jian Li*[1,2], *Fuyu Li*[1], *YaFei Jie*[1]

[1]Faculty of Metallurgical and Energy Engineering, Kunming University of Science and Technology, Kunming 650093, P. R. China
[2]State Key Laboratory of Complex Nonferrous Metal Resources Cleaning Utilization, Kunming, 650093, P. R. China
[*]E-mail: xucunying@kmust.edu.cn; xucunying@aliyun.com

Received: 8 December 2014 / *Accepted:* 9 January 2014 / *Published:* 19 January 2015

The electrochemistry of Ni(II) was studied with voltammetry and chronoamperometry at glass carbon (GC), mild steel (MS) and Pt electrodes in 1-ethyl-3-methylimidazolium (EMIC) ionic liquid with ethylene glycol. Cyclic voltammetry results shows that Ni(II) could be reduced to nickel metal via a single-step electron transfer process. However, the anodic dissolution of the nickel deposits was sluggish. In addition, the initial reduction potential of Ni(II) shifted positively as the temperature or concentration of Ni(II) increased. The diffusion coefficient of Ni(II) was estimated to be 4.6×10^{-7}cm^2 s^{-1}. The average activation energy for diffusion coefficient is about 21.75 kJ/mol. The electrodeposition of nickel proceeds via three-dimensional instantaneous nucleation with diffusion-controlled growth on both glassy carbon and Pt substrates. Smooth and dense Ni deposits can be obtained from EMIC ionic liquid with glycol.

Keywords: Ionic liquid; Nickel; Electrochemistry; Ethylene glycol

1. INTRODUCTION

The electrodeposition of nickel and its alloys has attracted much interest for their variety of commercial applications, such as decoration, corrosion and heat resistance, magnetic recording devices, etc[1–3]. Technological developments in recent years like micro-electromechanical systems require a better control of the morphology of the Ni and its alloy deposits[4–6]. Nickel and its alloys are generally electrodeposited from aqueous solutions. However, it is difficult to prevent hydrogen evolution, which leads to the low current efficiency and worse quality of deposits due to the hydrogen embrittlement[7-9]. Currently, the aspects of using ionic liquid electrodeposited metal has made great

progress[10]. The ionic liquids are expected to be the ideal alternative electrolyte for electrodeposition of various metals, since they posses unique chemical and physical properties such as wide electrochemical window, negligible vapor pressure, good conductivity, low melting point, wide temperature range for the liquid phase, and free from hydrogen evolution.

The electrodeposition of Ni has been mainly studied in acidic chloroaluminate or chlorozincate ionic liquids[11-20] except the $TFSA^-$ -based ($TFSA^-$: bis(trifluoro- methylsulfony) amid) and DCA^- -based (DAC^-: dicyanamide). In case of chloroaluminate or chlorozincate ionic liquids, the fact that aluminum is able to be electrodeposited on metals such as nickel, cobalt, and gold through underpotential deposition (UPD) makes it difficult to obtain pure Ni. Thus, the ionic liquids containing no metal species are promising for electrodeposition Ni and its alloy. Among the ionic liquid without metal species, 1-ethyl-3-methylimidazolium chloride (EMIC) ionic liquid is expected to be preferable for electrodeposition of various pure metal including Ni because this ionic liquid shows good ability to dissolve many metal compounds. Moreover, the addition of ethylene glycol (abbreviated EG) and glycerin (abbreviated G) in the electrolyte could improve the smoothness and color of the deposits and also increase the current efficiency[21]. However, the electrochemistry and electrodeposition of Ni has not been reported in this ionic liquid with EG. The understanding of the electrochemical behavior of Ni(II) is important for the control of the morphology and quality of Ni and its alloys. In this article, the electrochemical behavior of Ni(II) was investigated in a mixture of EMIC and EG (expressed as EMIC-EG solution) at various temperature.

2. EXPERIMENTAL

EMIC (Aldrich, 99.9%) was dried under vacuum at 353 K for 48 hours. Ethylene glycol (Sinopharm Chemical Reagent Co., Ltd. ≥99.0%) was dehydrated by molecular sieve. Anhydrous $NiCl_2$ (Sinopharm Chemical Reagent Co., Ltd. ≥99.0%) was heated up to 393 K and further dehydrated under vacuum for more than 10 hours. EMIC-EG solution was prepared by mixing EMIC ionic liquid and EG with molar ratio of 1:2 at 353 K. The bright green electrolyte was obtained by dissolving a certain amount of anhydrous $NiCl_2$ into the EMIC-EG solution.

All electrochemical experiments were conducted in a nitrogen gas-filled glove box (O_2 and H_2O < 5 ppm). The electrochemical experiments were accomplished using a Gamry PC14/300 electrochemical work station. A three-electrode electrochemical cell was used for all electrochemical experiments. The mild steel (MS) working electrode (geometric area 0.1256 cm^2) was made by inserting a piece of mild steel rod into a Teflon tube. The glassy carbon and platinum working electrode (geometric area 0.1256 cm^2) was purchased from Electroanalytical Systems. The MS electrode was polished successively with increasingly finer grades of emery paper followed by silicon carbide grit, and finally to a mirror finish with aqueous slurry of 0.05μm alumina, rinsed with distilled water, and dried under vacuum. The glassy carbon and platinum working electrode were polished with 0.05 μm alumina, rinsed with distilled water and finally dried under vacuum. Bulk electrodeposits were prepared on mild steel foils (1.0 × 0.5 cm, Aldrich). The counter electrode was a platinum spiral (Kunming Institute of Precious Metals, 99.99%) immersed in EMIC-EG solution. The reference

electrode was a Ag wire (Aldrich, 99.99%) placed in a separate fritted glass tube containing pure EMIC-EG solution of the same composition as the bulk solution. The electrolyte was heated to different experimental temperature between 333 and 363 K and allowed to stabilize at that temperature for 10-15 min. The deposition experiments were carried out by galvanostatic method.

The morphological characterization and elemental analysis of the Ni deposits were carried out using Philips XL30 scanning electron microscope (SEM). The phase analysis of the alloys electrodeposited was examined by a Rigaku D/max 2200 X-ray diffractometer (XRD) which uses monochromatic CuKα radiation (λ= 1.5406 Å).

3. RESULTS AND DISCUSSION

3.1 The cyclic voltammograms studies

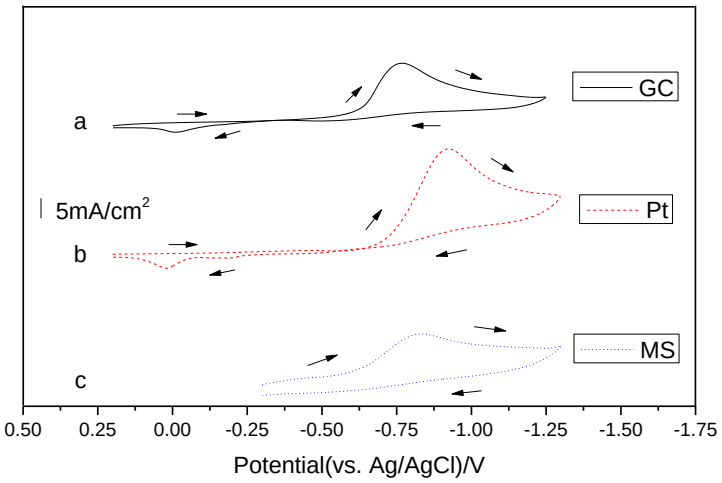

Figure 1. Cyclic voltammograms of 0.1 mol/L $NiCl_2$ in EMIC-EG solutions at different electrodes. The scan rate was 100 mV/s and temperature was 353 K.

Ni(II) was introduced into the EMIC-EG solution by dissolution of $NiCl_2$ at 353 K to give bright green solutions. The typical cyclic voltammograms (CVs) for the Ni(II) in the EMIC-EG solution at glassy carbon, steel mild, and platinum electrodes are shown in Fig. 1. Because the oxidation of iron occurs at a potential near that of nickel, the anodic scan was stopped before the stripping wave would occur. These voltammograms exhibits a single reduction wave with a peak potential around -0.7 V during the cathodic scan, and an oxidation wave with a peak potential around 0 V during the anodic scan. The reduction peak shown in Fig.1 is very broad and the integrated electric charges under the reduction peaks is larger than that integrated from the oxidation peak, suggesting the electrodeposited Ni during the cathodic scan could not be stripped completely during the anodic scan, probably because the concentration of Ni(II) near the electrode increased up to its saturated concentration quickly resulting in the hindrance of the anodic dissolution. The similar behavior has

been observed for the cyclic voltammetry of Ni in 1-butyl-3-methylpyrrolidinium bis(trifluoromethylsulfonyl) amide and 1-ethyl-3-methylpyrrolidinium dicyanamide. However, the electrodeposition of Ni at the mild steel electrode occurs at a potential more negative than that at the glassy carbon or Pt electrode. Furthermore, the current loop that is typical of deposition processes requiring nucleation overpotential is apparent in the voltammogram recorded at glassy carbon electrodes. No notable nucleation overpotential feature is observed in the voltammogram recorded at the mild steel and Pt electrode. These results indicate that the electrodeposition of Ni may more facile at mild steel electrode than at the glassy carbon and Pt electrodes.

The cathodic peak potential shifted negatively and the peak current increased as the scan rate was increased (see supporting information). The typical data resulting from a series of cyclic voltammetric experiments at different scan rates, ν, are collected in Table 1. The values for $|E_{pc} - E_{pc/2}|$, where E_{pc} is peak potential and $E_{p/2}$ is half-peak potential, are larger than the theoretical value of 0.012 V expected for a reversible two-electron electrode process at 353 K. Overall, these results suggest that the Ni(II) reduction is quasi-reversible at glassy carbon, mild steel and platinum substrates. Similar quasi-reversible behavior was previously found for Cd(II) in a acidic $ZnCl_2$-EMIC melt[22] and for Sn(II) and Zn(II) in acidic $AlCl_3$-EMIC melts.

At the glassy carbon, mild steel and Pt electrodes, the peak current (*I*p) increases linearly with the increasing of the square root of the potential scan rate ($v^{1/2}$), which suggests Ni deposition process is mainly controlled by diffusion[11]. The diffusion coefficient of the Ni(II) can be estimated to be $4.6\times10^{-7}cm^2/s$ according to the Eqs. (1) and (2)[23].

$$|E_p - E_h| = \frac{1.857RT}{\partial n_\partial F} \quad (1)$$

$$i = 0.496nFCAD^{\frac{1}{2}}\left(\frac{(\partial n_\partial)Fv}{RT}\right)^{\frac{1}{2}} \quad (2)$$

where ∂, n, i, c, A and D mean transfer constant, electron transfer number, reduction peak current, concentration of Ni(II), electrode area and diffusion coefficient, respectively.

Table 1. Summary of voltammetric data for the reduction of 0.1 mol L^{-1} Ni (II) at different stationary electrode at 353 K

electrode	*V* (mV/s)	E_p (V)	E_h (V)	$\lvert E_p-E_{p/2}\rvert$(V)	i_p(A·cm^{-2})	$i_p/v^{1/2}$(A s$^{1/2}$ V$^{1/2}$)
GC	10	-0.675	-0.610	0.065	6.05×10^{-4}	0.00605
	25	-0.702	-0.625	0.077	9.60×10^{-4}	0.00607
	50	-0.731	-0.648	0.083	1.35×10^{-3}	0.00603
	75	-0.751	-0.663	0.098	1.65×10^{-3}	0.00602
	100	-0.768	-0.681	0.087	1.94×10^{-3}	0.00614
Pt	10	-0.771	-0.705	0.066	1.04×10^{-2}	0.10347
	25	-0.822	-0.747	0.075	1.57×10^{-2}	0.09936
	50	-0.870	-0.780	0.090	2.06×10^{-2}	0.09196
	75	-0.901	-0.798	0.103	2.41×10^{-2}	0.08796
	100	-0.923	-0.815	0.108	2.77×10^{-2}	0.08766
MS	10	-0.754	-0.683	0.071	6.04×10^{-4}	0.00604

	25	-0.784	-0.694	0.090	9.14×10^{-4}	0.00578
	50	-0.813	-0.710	0.103	1.29×10^{-3}	0.00576
	75	-0.824	-0.709	0.115	1.55×10^{-3}	0.00566
	100	-0.832	-0.712	0.120	1.76×10^{-3}	0.00557

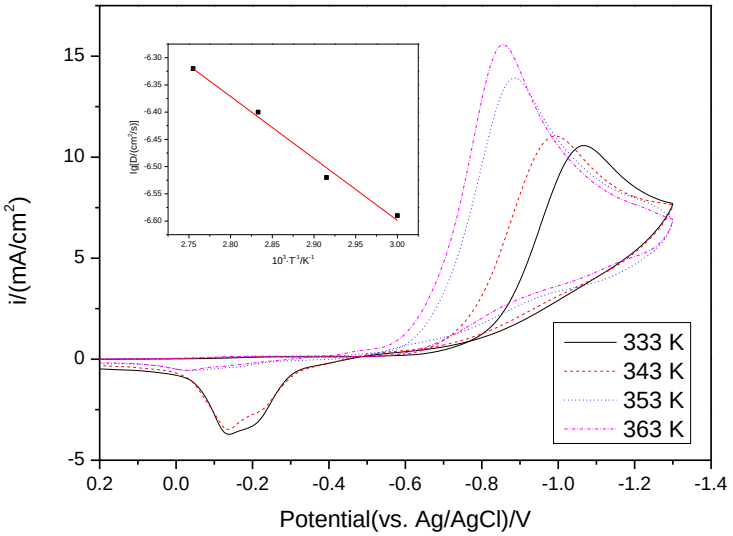

Figure 2. Cyclic voltammograms of GC electrode in EMIC-EG solution containing 0.1 mol/L $NiCl_2$ at different temperature. The scan rate was 200 mV s^{-1}. The insert shows the dependence of the logarithm of the diffusion coefficient on the reciprocal of temperature

Fig. 2 shows the cyclic voltammograms of a glassy carbon electrode in the EMIC-EG solution containing $NiCl_2$ (0.1 mol/L) at various temperatures. The reduction peak current (i_p) increased, the potential of reduction peak shifted positively and the separation between the reduction and oxidation peaks became smaller with elevating temperature, indicating that reaction rate increased and overpotential for electrodeposition of Ni in EMIC-EG solution decreased at higher temperature. This is not surprising because at higher temperature the charge transfer and mobility of the electroactive species will increase while the nucleation overpotential will be decrease. According to the method mentioned above, the diffusion coefficients at different temperatures were estimated and shown in Table 2. The diffusion coefficient increased with elevating temperature, obeying the Arrhenius′ law as follow:

$$\lg D = -\frac{E_D}{2.303RT} + C \qquad (3)$$

Where D is diffusion coefficient, T is the absolute temperature, E_D is diffuction activation energy, R is gas constant and C is constant term. From the dependence of the logarithm of the diffusion coefficient on the reciprocal of temperature shown in Fig.2 (inserted), the diffusion activation energy of Ni(II) in EMIC-EG containing $NiCl_2$ (0.1 mol/L) is caculated to be 21.75 kJ/mol, which is close to that in BMPTFSA ionic liquid containing 0.1 mol/L $NiCl_2$ (26 kJ/mol)[24]. It is well known that the electrode reaction is controlled by diffusion when activation energy is less than 40 kJ/mol[25].

This result again illustrated that Ni deposition process was mainly controlled by diffusion in EMIC-EG solution containing $NiCl_2$ (0.1 mol/L).

Table 2. The diffusion coefficient at different temperature

T/K	335	345	355	365
D/×$10^{-7}$$cm^2$/s	2.55	3.03	3.96	4.78

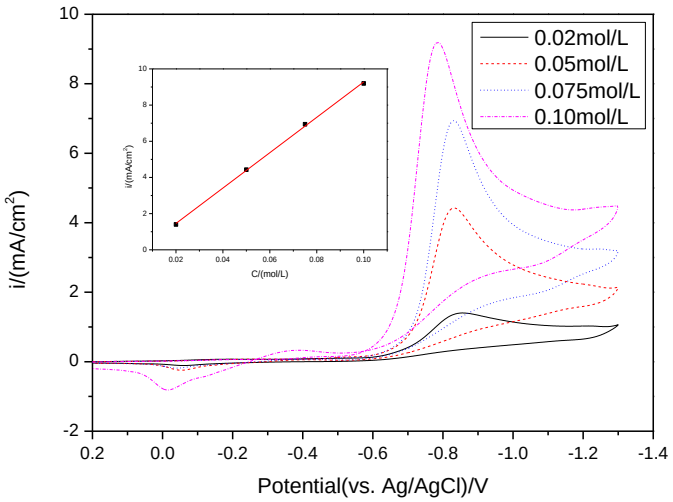

Figure 3. Cyclic voltammograms recorded at glassy carbon electrode in EMIC-EG solution containing various concentration of Ni(II). The scan rate was 25 mV s^{-1} and temperature is 353 K. The inset shows the linear relationship between reduction peak current (I_{pc}) and Ni(II) concentration

Fig. 3 shows the cyclic voltammograms recorded at glassy carbon electrode for solution containing different concentration of Ni(II) from 0.02 to 0.10 mol L^{-1}. As shown in Fig. 3, the reduction potential shifted positively and the reduction peak current increased with increasing of the Ni(II) concentration. When the cathodic peak current, i_p, was plotted against the Ni(II) concentration, a linear relationship between i_p and Ni(II) concentration is observed as shown in the inset of Fig. 3. These results indicate that the deposition of Ni becomes more facile with increasing of Ni(II) concentration.

3.2 Nucleation and growth of nickel electrodeposition

To further study the nucleation/growth process for the electrodeposition of Ni(II), chronoamperometry experiments were performed at glassy carbon and Pt, and mild steel electrodes. These experiments were carried out by stepping the potential of the working electrode from a value where no reduction of Ni(II) would occur to potentials sufficient negative to initiate nucleation/growth process after a short induction time. It was found that in the 25-75 mol % EMIC-EG solution, the Ni

nucleation occurred with an extremely short induction time and the experimental current-time transients were not very reproducible at all the three electrodes. Similar behavior was also observed at the Ni electrode in the 50.0-50.0 mol % $ZnCl_2$-EMIC melt. Thus, only the results obtained at glassy carbon and Pt electrodes in the 25-75 mol % EMIC-EG solution are discussed.

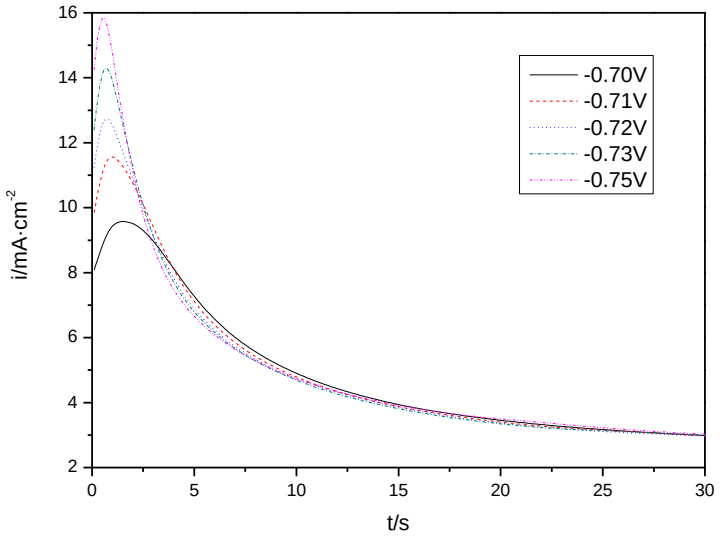

(a) GC electrode

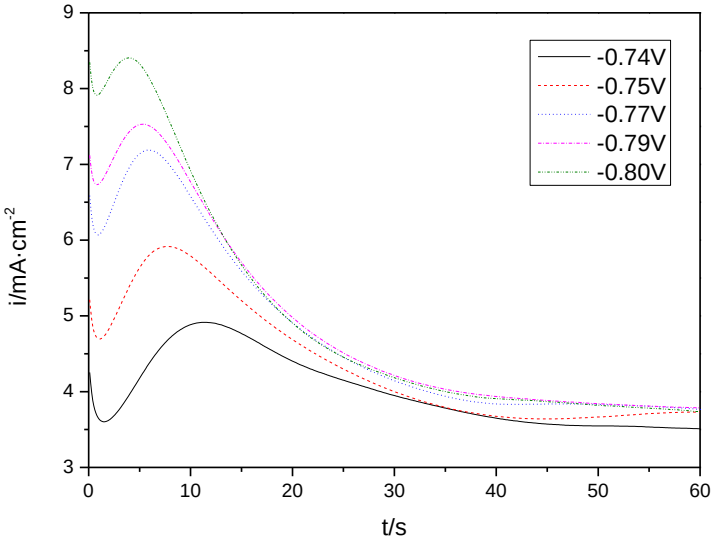

(b) Pt electrode

Figure 4. Current-time transients of the chronoamperometric experiments recorded at (a) glassy carbon and (b) Pt electrodes for 0.1 mol L^{-1} Ni(II) species in the EMIC-EG solution. The temperature is 353 K

Fig. 4 displays the typical current-time transients from the chronoamperometry experiments for nickel deposition in the EMIC-EG solution at glassy carbon and Pt electrodes. These transients all exhibit the classic shape for a three-dimensional nucleation process: after the decay of a sharp electrode double-layer charging current, the faradaic current increases due to the nucleation and growth of Ni nuclei. This rising current eventually reaches a current maximum, i_m, as the discrete diffusion

zones for each of the growing crystallites begin to overlap at time t_m. After time t_m, the current starts to decay due to the increase of the diffusion layer thickness.

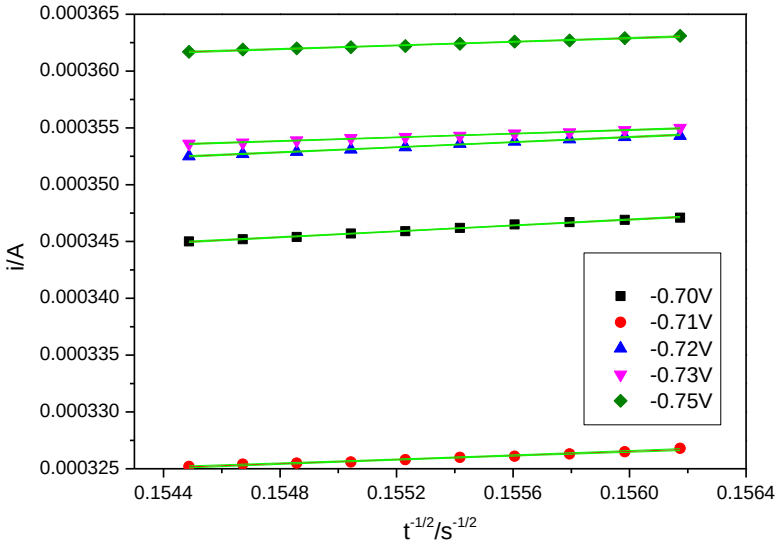

(a) GC electrode

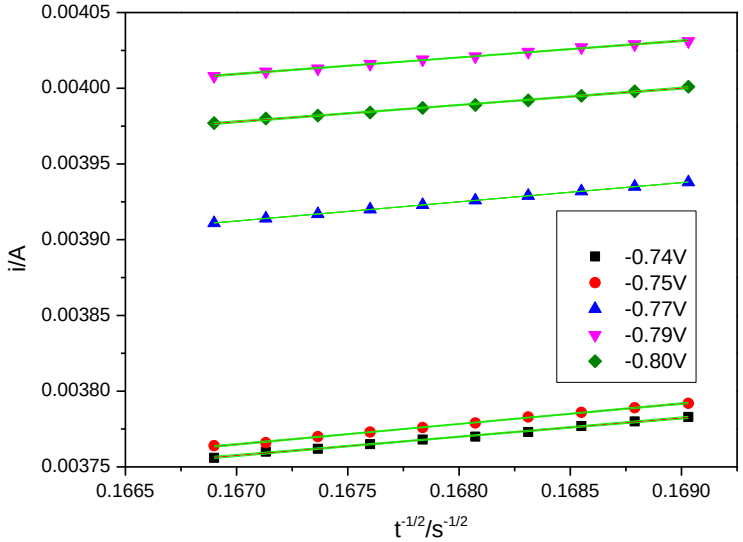

(b) Pt electrode

Figure 5. The current varies linearly with the reciprocal of square root of the time

Examining the current-time transients in Fig. 4 reveals that the nucleation/growth process of Ni at glassy carbon electrode reaches t_m faster than at Pt electrode, and the values of the i_m observed at glassy carbon are in general higher than those observed at Pt. These observations suggest that the nucleation/growth of Ni occurs at glassy carbon substrate more readily than at Pt substrate. It can also be seen in Fig. 4 that after current maxima (t_m), all the current transients decayed slowly and, for a longer time, almost merged into a common curve, which was caused by diffusion control and can be described by the Cottrell equation as follows[26]:

$$i = -\frac{nFAD^{1/2}C}{\pi^{1/2}t^{1/2}}$$

where i is the current density, n is the number of electrons involved, F is the Faraday constant, D is the diffusion coefficient, C is the concentration of species in the bulk, and t is time. On the basis of the Cottrell equation, the diffusion coefficients of Ni(II) in EMIC-EG media were also estimated by analyzing the part after the maximum of current transients. The current varies linearly with the reciprocal of square root of the time as shown in the Fig. 5. Accordingly, The diffusion coefficient for Ni(II) in EMIC-EG solution was caculated to be 5.36×10^{-7}cm^2 s^{-1}, which was in good with that from cyclic voltammograms. The value of diffusion coefficient for Ni(II) is approximate to or smaller than that obtained in the $AlCl_3$-EMIC (2.1×10^{-7} cm^2 s^{-1}[27]and 2.8×10^{-6} cm^2 s^{-1}[28]) and [Emim]DCA (2.1×10^{-6} cm^2 s^{-1}[29]) ionic liquid.

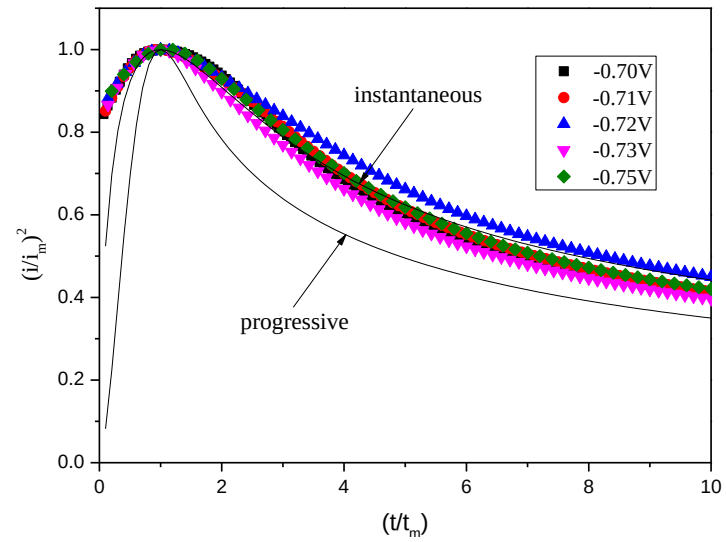

(a) GC electrode

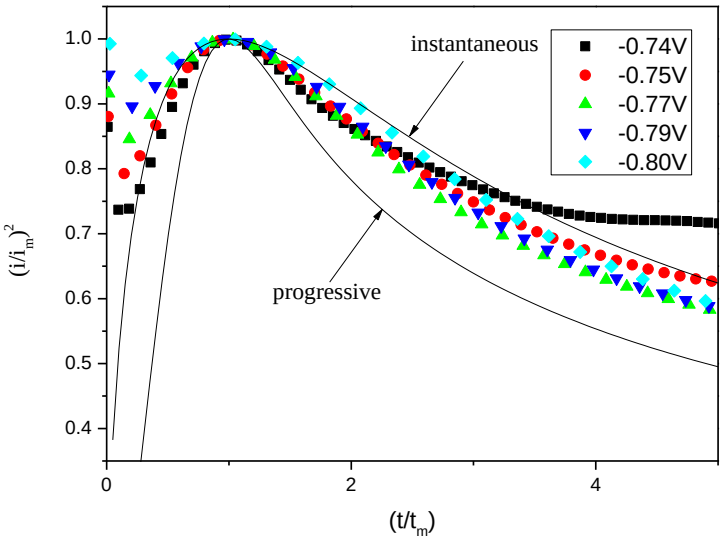

(b) Pt electrode

Figure 6. Comparison of the dimensionless experimental current-time transients derived from the chronoamperometric experiments for 0.1mol L^{-1} Ni(II) species in the EMIC-EG solution at (a) glassy carbon and (b) Pt electrodes. The temperature is 353 K.

The experimental current-time transients can be expressed in normalized dimensionless forms to generate plots of $(i/i_m)^2$ vs. (t/t_m). These experimental plots are compared to the theoretical dimensionless current transients derived for the case of three dimensional instantaneous (Eq.(4)) and progressive (Eq.(5)) nucleation, respectively[30]:

$$(i/i_m)^2 = 1.9542\{1-\exp[-1.2564(t/t_m)]\}^2(t/t_m)^{-1} \quad (4)$$

$$(i/i_m)^2 = 1.2254\{1-\exp[-2.3367(t/t_m)^2]\}^2(t/t_m)^{-1} \quad (5)$$

The experimental and theoretical plots are shown in Fig. 6. It is apparent from this figure that the electrodeposition of Ni at both glassy carbon and Pt substrates follows the three-dimensional instantaneous nucleation/growth process. This behavior is different from that observed for the electrodeposition of Ni in the [EMIm]DCA and Lewis acidic $AlCl_3$-EMIC ionic liquid , in which the reduction of Ni proceeded via three-dimensional progressive nucleation/growth[29,31].

3.3 Electrodeposition of Ni

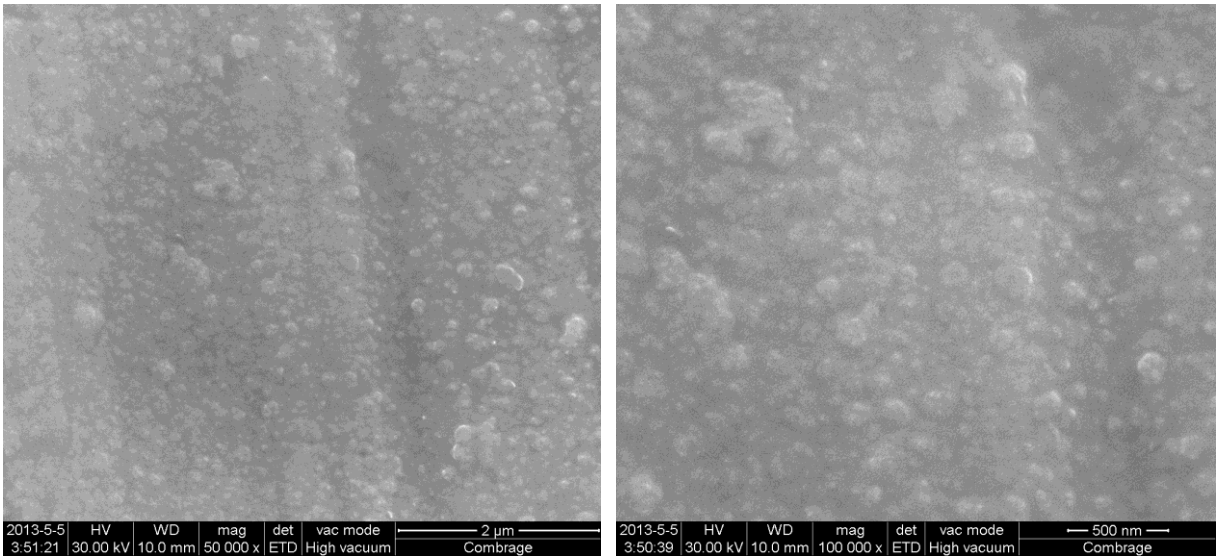

Figure 7. SEM micrographs of the deposit

The electrodeposition of Ni on a mild steel substrate in EMIC-EG containing 0.1 mol L^{-1} Ni(II) was performed by galvanostatic electrolysis with the current density of 1mA cm^{-2}. In the electrodepositing experiments, a Ni sheet was immersed in the electrolytic solution as the counter electrode in order to compensate for the consumption of Ni specious. A smooth and adhesive electrodeposit with slight brightness was obtained. Fig. 7 shows the SEM image of the deposit. The deposits are dense and the particle sizes were under 100 nm. The particle size of deposit was significantly smaller than that obtained in BMPTFSA ionic liquid by galvanostatic electrolysis[32] and in [BMIm]DCA by potentiostatic electrolysis[29].The X-ray diffraction pattern for the deposits is shown in Fig.8. All XRD peaks are indexed to Ni and Fe substrate, which indicates that the deposits are mainly composed of Ni. The X-ray reflection of Ni broadening was observed, suggesting the grain

size of the Ni deposit is very small. This result is consistent with the SEM analysis (Fig. 7). Moreover, XRF analysis showed that the deposit was mainly composed of Ni.

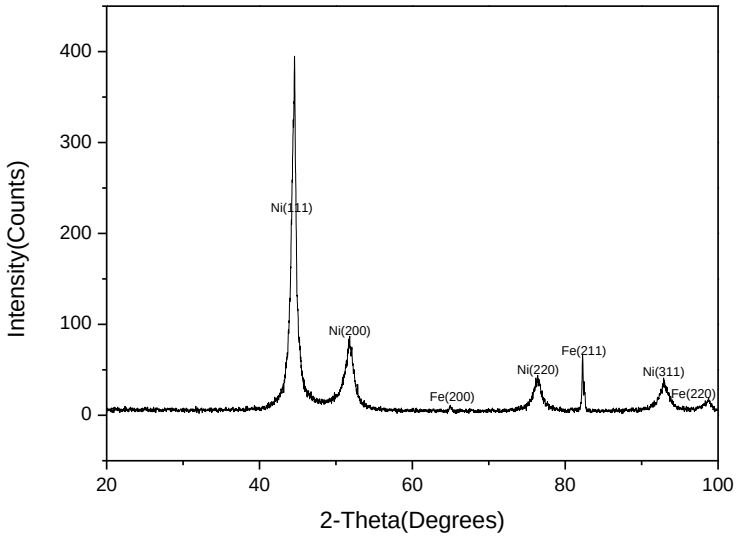

Figure 8. The XRD pattern of Ni deposits

4. CONCLUSIONS

The electrochemistry of Ni(II) was investigated in the EMIC ionic liquids with EG (EMIC-EG solution). Ni(II) could be reduced to nickel metal via a single-step electron-transfer process. In contrast to the three-dimensional progressive nucleation/growth that was observed for the electrodeposition of Ni in the [EMIm]DCA and Lewis acidic $AlCl_3$-EMIC ionic liquid, the electrodeposition of Ni in EMIC-EG solution at both Pt and glassy carbon substrates involves three-dimensional instantaneous nucleation/growth. The growth of Ni nuclei at Pt and glassy carbon is diffusion limited. The diffusion coefficient of Ni(II) in EMIC-EG solution is $(4.6\pm1.1)\times10^{-7}cm^2\ s^{-1}$ from cyclic voltammograms and chronoamperometric are approximate to or smaller than that obtained in the $AlCl_3$-EMIC and [EMIm]DCA ionic liquid. The average activation energy for diffusion coefficient is about 21.75 kJ/mol. The obtained deposits on steel mild substrate are dense and smooth. This results revealed in this study indicate that EMIC-EG solution can be a promising electrolyte for the electrodeposition of various Ni alloys.

ACKNOWLEDGEMENT
The authors gratefully acknowledge the financial support of the National Natural Science Foundation of China (Project No. 21263007, 51274108).

References

1. F. F. Miranda, O. E. Barcia, O. R. Mattos, R. Wiart, *J. Electrochem. Soc.*, 144 (10) (1997) 3441-3449.
2. G. Roventi, R. Fratesi, R. A. Delle Guardia, G. Barucca, *J. Appl. Electrochem.*, 30 (2) (2000) 173-

179.
3. M. M. Abou-Krisha, *Appl. Surf. Sci*., 252 (4) (2005) 1035-1048.
4. M. Metikos-Hukovic, I. Skugor, Z. Grubac, R. Babic, *Electrochim. Acta.*, 55 (9) (2010) 3123-3129.
5. U. S. Mohanty, B. C. Tripathy, P. Singh, S. C. Das, *J. Electroanal. Chem*., 526 (1-2) (2002) 63-68.
6. W. W. Chen, W. Gao, *Electrochim. Acta.*, 55 (2010) 6865.
7. A. M. Alfantazi, A. Shakshouki, *J. Electrochem. Soc*., 149 (10) (2002) C506-C510.
8. C. Lupi, M. Pasquali, A. Dell'Era, *Miner. Eng*., 19 (12) (2006) 1246-1250.
9. M. J. Deng, I. W. Sun, P. Y. Chen, J. K. Chang, W. T. Tsai, *Electrochim. Acta*., 53 (19) (2008) 5812-5818.
10. P. X. Yang, M. Z. An, S. M. Liang, *ELECTROPLAT & POLLUT CONTROL*, 26 (5) (2006) 1-5.
11. C. A. Zell, W. Freyland, *Chem. Phys. Lett.*, 337 (2001) 293.
12. S. P. Gou, I. W. Sun, *Electrochim. Acta.*, 53 (2008) 2538.
13. O. Mannetal, G. B. Pan, W. Freyland, *Electrochim. Acta.*, 54 (2009) 2487.
14. R. J. Gale, B. Gilbert, R. A. Osteryoung, *Inorg. Chem.*, 18 (1979) 2723.
15. R. P. William, C. L. Hussey, *J. Electrochem. Soc.*, 143 (1996) 130.
16. T. P. Moffat, *J. Electrochem. Soc.*, 141 (1994) 3059.
17. O. Mann, W. Freyland, *J. Phys. Chem. C*, 111 (2007) 9832.
18. M. R. Ali, A. Nishikata, T. Tsuru, *J. Electroanal. Chem.*, 513 (2001) 111.
19. W. Freyland, C. A. Zell, S. Z. E. Abedin, *Electrochim. Acta.*, 48 (2003) 3053.
20. T. C. Richard, *J. Electrochem. Soc.*, 145 (1998) 1598.
21. J. D. Ma, B. Li, L. G. Yan, *Nonferrous Met.*, 2 (2010) 62-66.
22. J. F. Huang, I. W. Sun, *J. Electrochem. Soc*., 149 (9) (2002) E348-E355.
23. A. J. Bard, L. R Faulkner, *Electrochemical Methods-Fundamentals and Applications*, Wiley, New York (1980).
24. Y. L. Zhu, Y. Kozuma, Y. Katayama, *Electrochimica Acta.*, 54 (28) (2009) 7502-7506.
25. H. Y. Jiang, *Metallurgical electrochemistry*, Beijing: Metallugical Industry Press, (1983).
26. F. G. Cottrell, *Z Physik Chem.*, 42 (1902) 385.
27. O. Mann, W. Freyland, *J. Phys. Chem. C*, 111 (2007) 9832.
28. W. R. Pitner, C. L. Hussey, G. R. Stafford, *J. Electrochem. Soc.*, 143 (1996) 130.
29. M. J. Deng, I. Sun, P. Y. Chen, *Electrochim. Acta*., 53(19) (2008) 5812-5818.
30. B. R. Scharifker, G. Hills, *Electrochim. Acta.*, 28(7) (1983) 879-889.
31. W. R. Pitner, C. L. Hussey, *J. Electrochem. Soc*., 144 (9) (1997) 3095-3103.
32. Y. L. Zhu, Y. Katayama, T. Miura, *Electrochim. Acta*,, 123 (2014) 303-308.

SUPPORTING INFORMATION:

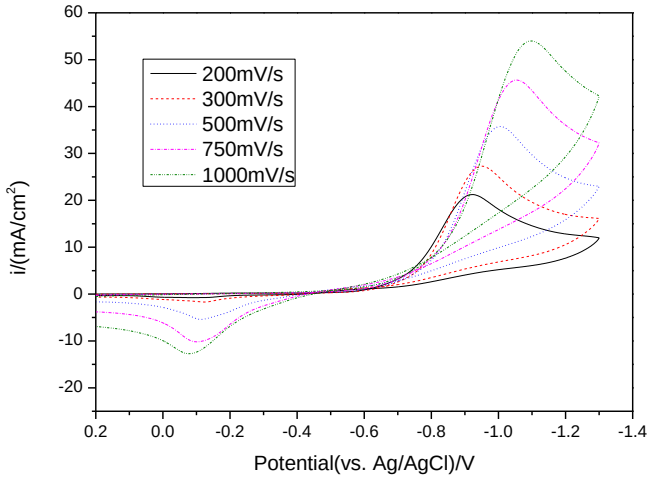

Figure 1S. Cyclic voltammograms of glassy carbon electrode in EMIC-EG solution containing 0.1 mol/L $NiCl_2$ at different scan rate. The temperature was 353 K.

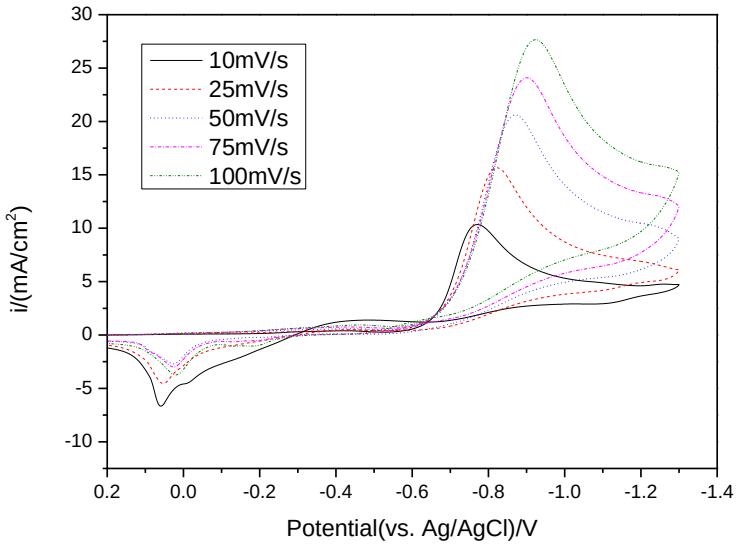

Figure 2S. Cyclic voltammograms of Pt electrode in EMIC-EG solution containing 0.1 mol/L $NiCl_2$ at different scan rate. The temperature was 353 K.

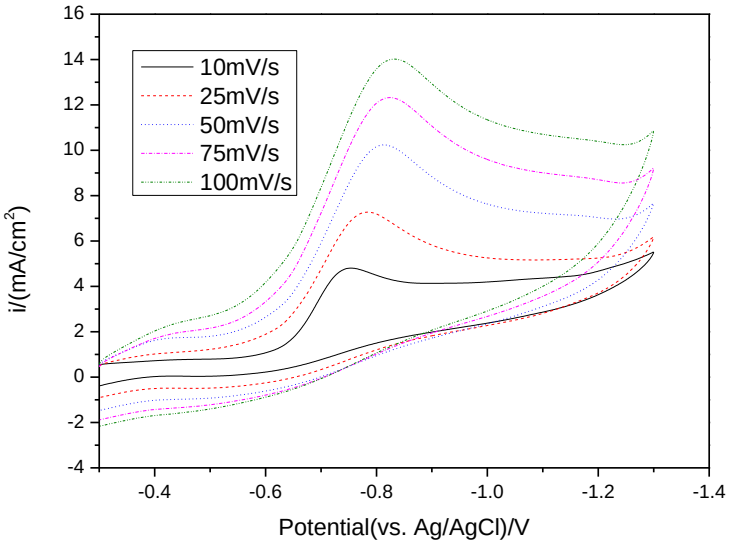

Figure 3S. Cyclic voltammograms of mild steel electrode in EMIC-EG solution containing 0.1 mol/L $NiCl_2$ at different scan rate. The temperature was 353 K.